Send Orders for Reprints to reprints@benthamscience.ae

Current Pharmaceutical Design, 2018, 24, 576-594

RESEARCH ARTICLE

Virtual Screening and Statistical Analysis in the Design of New Caffeine Analogues Molecules with Potential Epithelial Anticancer Activity

Josivan da Silva Costa*[,a,b,c], Karina da Silva Lopes Costa[b], Josiane Viana Cruz[b], Ryan da Silva Ramos[b], Luciane Barros Silva[b], Davi Do Socorro Barros Brasil[c], Carlos Henrique Tomich de Paula da Silva[d], Cleydson Breno Rodrigues dos Santos[b] and Williams Jorge da Cruz Macêdo[e]

[a]*Postgraduate Program in Biotechnology and Biodiversity-Network BIONORTE, Federal University of the Pará, Belém, Brazil;* [b]*Laboratory of Modeling and Computational Chemistry, Federal University of Amapá, Department of Biological Sciences. Rod. Juscelino Kubitschek, Km 02, s/n, Jardim Marco Zero, 68902-280 Macapá-AP, Brazil;* [c]*Institute of Technology, Federal University of Pará, Av. Augusto Corrêa, 01, Belém, Pará 66075-900, Brazil;* [d]*Computational Laboratory of Pharmaceutical Chemistry, Faculty of Pharmaceutical Sciences of Ribeirão Preto, University of São Paulo, Ribeirão Preto, São Paulo, Brazil;* [e]*Laboratory of Molecular Modeling and Simulation System, Federal Rural University of Amazônia, Rua João Pessoa, 121, Campus Capanema-Centro, Capanema, Pará 68700-030, Brazil*

ARTICLE HISTORY

Received: April 6, 2016
Accepted: June 30, 2016

DOI:
10.2174/1381612823666170711112510

Abstract: About 132 thousand cases of melanoma (more severe type of skin cancer) were registered in 2014 according to the World Health Organization. This type of cancer significantly affects the quality of life of individuals. Caffeine has shown potential inhibitory effect against epithelial cancer. In this study, it was proposed to obtain new caffeine-based molecules with potential epithelial anticancer activity. For this, a training set of 21 molecules was used for pharmacophore perception procedures. Multiple linear regression analyses were used to propose mono-, bi-, tri-, and tetra-parametric models applied in the prediction of the activity. The generated pharmacophore was used to select 350 molecules available at the ZINCpharmer server, followed by reduction to 24 molecules, after selection using the Tanimoto index, yielding 10 molecules after final selection by predicted activity values > 1.5229. These ten molecules had better pharmacokinetic properties than the other ones used as reference and within the clinically significant limits. Only two molecules show minor hits of toxicity and were submitted to molecular docking procedures, showing BFE (binding free energy) values lower than the reference values. Statistical analyses indicated strong negative correlations between BFE and pharmacophoric properties (high influence on BFE lowering) and practically null correlation between BFE and BBB. The two most promising molecules can be indicated as candidates for further *in vitro* and *in vivo* analyzes.

Keywords: Epithelial cancer, caffeine, Chk1, Molecular modeling, multiple linear regression, Pharmacokinetic and toxicological properties.

1. INTRODUCTION

Cancer is a disease characterized by the abnormal cell growth in an organism; it is also known as malignant neoplasm or malignant tumor. It can be caused by chemical, physical and biological agents and has its origin in genetic alterations of cells. The main effects observed in neoplastic cells are loss of function resulting from the absence of differentiation, uncontrolled proliferation, invasion of adjacent tissues and metastasis [1-3].

There are several types of cancer depending on which region of the body is affected. Diagnoses of cancer worldwide show that the most common are lung cancer, with 1.8 million cases, 1.7 million breast of breast cancer and uterine cervix and rectum cancer with 1.4 million. Regarding skin cancer, it is estimated that melanoma alone (the most aggressive of skin tumors) has an incidence of around 132 thousand cases per year, most of them registered in tropical areas [4].

Also known as epithelial cancer, skin cancer is primarily caused by the incidence of UVB rays, in addition to being influenced by the individual's lifestyle [5]. Skin cancer receives several nomenclatures, which depends on which layer of skin the cancer develops, and can be of two types: non-melanomas - Basal Cell Carcinoma (BCC) and Squamous Cell Carcinoma (SCC); And melanoma - cutaneous malignant melanoma that originates in melanocytes, melanin-producing cells, and has high potential to generate metastases [6].

The anticancer action of plant substances has been widely studied, among them there are studies related to caffeine acting as epithelial anticancer agent. Such as the effect of caffeine as a radiosensitizer on cancer cells [7], the effect of caffeine on rat skin irradiated by UVB rays [8] and the effect of caffeine and analogues on the growth of epidermal cells of rats of the JB6 P + lineage [9]. Caffeine (1,3,7-trimethylxanthine) is an alkaloid compound belonging to the xanthine group, presents basic character and of plant origin, it contains in its composition nitrogen, oxygen, hydrogen and carbon [10].

Regarding the biological receptor responsible for the epithelial anticancer action, when such neoplasia is caused by the UVB incidence, Sarkaria *et al.* (1999) [7] indicate that methylxanthines inhibit a phosphotransferase kinase protein required for checkpoint signaling in cells with damaged DNA and that the possible action of trialkylxanthines on protein kinases can be attributed to a prominent target candidate: Chk1. The reference to this possible target was also made by Lu *et al.* (2008) [8], where they consider that the key to the pro-apoptotic effect of caffeine in the epidermis of mice exposed to UVB is in the inhibition of the signal transduction pathway UVB → ATR → Chk1 → cdc25c → cdc2 → cdc2 / Cyclin B1. The presence of caffeine stimulates UVB-induced apoptosis, inhibits phosphorylation of Chk1 over Ser345, and restricts the decrease of mitotic cells acting on cyclin B1 (which occurs shortly after UVB irradiation).

*Address correspondence to this author at the Laboratory of Modeling and Computational Chemistry, Federal University of Amapá, Department of Biological Sciences. Rod. Juscelino Kubitschek, Km 02, s/n, Jardim Marco Zero, 68902-280 Macapá-AP, Brazil; Tel: +55(96)991639638;
E-mail: josivan.chemistry@gmail.com

In this study, information on the biological receptor Chk1 [7, 8] and data of molecular structures and ICT_{50} from 30 molecules, selected from the literature [9], were used to perform virtual screening (diagram shown in Fig. **1**) to obtain new caffeine analog molecules with epithelial anticancer activity.

2. MATERIALS AND METHODS

2.1. Data Set Selection

We selected 30 molecules derived from trialkylxanthine with experimental values of biological activity [9] related to the prevention of Epidermal Growth Factor (EGF) in the malignant transformation of epidermal cells of susceptible JB6 rats (P +) C141 (JB6 P +). Activity values were presented as ICT_{50} (50% inhibition of cell transformation) against epithelial cancer.

The training set molecules used for the construction of the pharmacophore model were selected in decreasing biological activity sequence (from 0.01 to 0.24 mM), containing the most active, since the activity is a critical factor for the determination of the pharmacophore characteristics and for the validation of the model Multiple Linear Regression (MLR) [11, 12]. Caffeine and xanthine molecules were introduced in the training set, according to the following considerations: (1) introduction of caffeine, here used as the reference/prototype molecule; (2) introduction of xanthine, because it has the active scaffold of the molecules here investigated. A total of 21 molecules comprise of the final training set.

The test set comprised 9 molecules randomly selected, which was here used for external validation of the MLR model. Structures were drawn using the ChemScketch software [13] and saved in the mol format, except caffeine, for which the crystallographic pose was retrieved from the Cambridge Structural Database portal at http://webcsd.ccdc.cam.ac.uk/. Both files were later.

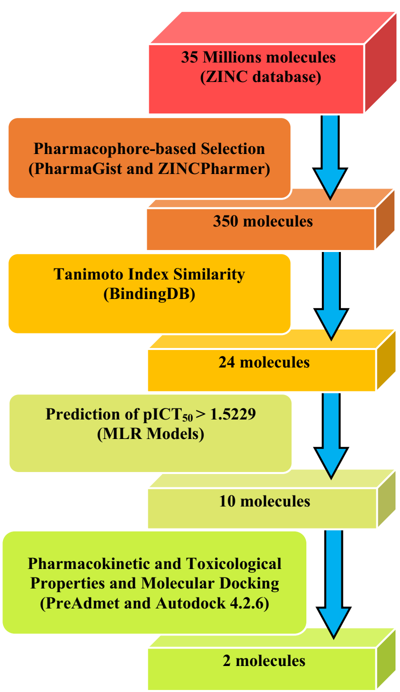

Fig. (1). Flowchart of the virtual screening of new caffeine analog molecules with potential epithelial anticancer activity.

converted to mol2 using the Open Babel tool 2.3.2 [14]. The geometries of the molecules were optimized according to the Molecular Mechanics MM+ Force Field, using the HyperChem 7 program [15].

2.2. Pharmacophore Model Perception

The mol2 files of the training set were inserted into the PharmaGist online server [16] to generate the pharmacophoric pattern of caffeine and analogues, with caffeine as pivot (keeped frozen) structure. PharmaGist generates a pharmacophore model based on the overlapping of individual pharmacohoric groups of input ligands (the training set). The method essentially aligns and overlaps the molecules with a pivot (the caffeine molecule) seeking a set of chemical and spatial characteristics that are common to the largest possible number of the input ligands. Assemblies with higher scores and with higher number of aligned ligands are considered better candidates for pharmacophoric models [16, 17].

2.3. Building and Validation of MLR Models

This step is crucial to evaluate the efficiency and predictive ability of MLR models in accurately identifying new active molecules. Pharmacophoric models indicated by PharmaGist were characterized according to their physicochemical and structural properties, such as: Number of atoms (A), general characteristics (GF), Spatial characteristics (SF), Aromatic region (Ar), Hydrophobic region (Hyd), hydrogen bond donor (Don), hydrogen bond receptor (Acc), anion (Neg) and cation (Pos). These characteristics were used to calculate the theoretical $pICT_{50}$ values from multiple linear regression of the pharmacophoric characteristics of the molecules of the training set against the experimental $pICT_{50}$ values.

Pearson's correlation was used to identify the relationship between the pharmacophoric properties of the 21 molecules in the training set associated with $pICT_{50}$ values. The correlation cutoff was 0.3 according to previous studies conducted by Santos *et al.* (2015) [18]. After identifying the main pharmacological properties associated with biological activity, mono, bi, tri and tetra-parametric models were developed.

The experimental ICT_{50} values were converted to $pICT_{50}$ in order to reduce inconsistencies caused by the statistical steps, with the equation (1): $pICT_{50} = -\log ICT_{50}$. The $pICT_{50}$ values were predicted for the training set, test set and triaged molecules as well, by the application of the MLR models. The MLR analyses are implemented in the Statistica 7 program [19].

Data of the pharmacophoric characteristics of the test set molecules were obtained from the PharmaGist web server by the same previous way for the training set, except for the indication of a pivot molecule, where it was now selected automatically by the server itself.

2.4. Virtual Sorting in ZINCPharmer

The best pharmacophore file obtained in PharmaGist for caffeine and analogues was inserted in the ZINCPharmer web server, available at http://zincpharmer.csb.pitt.edu/ [20]. This tool performs a virtual screening from the ZINC database [20, 21], a database with approximately 35 million structures of commercially available compounds.

2.5. Tanimoto Similarity Search

The structures obtained from ZINCPharmer were selected by Tanimoto's similarity search procedure via the BindingDB web server. Molecules with similarity values greater than 0.6 were selected [22]. For this selection, 12 molecules (xanthine, caffeine and ten most active) compose reference set. Theoretical $pICT_{50}$ values were calculated for the molecules obtained from the Tanimonoto test, using the MLR models. Pharmacological data for ZINC molecules were obtained in the same manner as described for both the training set and test set.

2.6. Determination of Pharmacokinetic and Toxicological Properties

This step was performed after setting a cut-off point from the $pICT_{50}$ values of the five most active molecules of the training set.

The resulting molecules were analyzed in the Derek software [23] (Toxicologic properties) and in the online Preadmet tool available at https://preadmet.bmdrc.kr/, This tool was used to determine selected pharmacokinetic properties (Human Intestinal Absorption - HIA, Plasma Protein Binding - PPB and Blood Brain Barrier - BBB) and toxicological (Mutagenicity and Carcinogenicity).

2.7. Molecular Docking Study

2.7.1. Selection of a Receptor-Ligand Complex Used in Molecular Docking

The selection of the Chk1 receptor was based on the propositions by Sarkaria *et al.* (1999) [7] and Lu *et al*. (2008) [8] (as previously discussed), highlighting the Chk1 receptor as a prominent target for the action of alkylxanthines against epithelial cancer.

The Protein Data Bank (PDB) provides several receptor-ligand complex alternatives for Chk1. However, the structure of this receptor complexed with caffeine is not available in the PDB, which makes it necessary to select the receptor-ligand complex (for further docking) as described below:

Selection of the receptor-ligand complex Chk1 (target protein) was performed taking into account (1) the structural similarity (visual inspection) of the ligands to the xanthine scaffold structure, regarding the presence of the heterocyclic rings; followed by (2) the overlap of the ligands with the caffeine structure, in relation to the overlap similarity values.

For PDB selection, only small ligand structures (characteristic common to the molecules here studied) from target in complex with only one ligand were selected. The structural similarity was accessed in the Discovery Studio 4.0 Client tool [24]. The ligands obtained were analyzed regarding the overlap similarity with caffeine.

2.7.2. Molecular docking of the most promising ZINC molecules

Initially, the receptor Chk1 file (ID: 2WMR, with resolution of 2.43 Å), chosen from the best caffeine overlapping ligand, was obtained from the PDB at http://www.rcsb.org/pdb/home/home.do [25], complexed with 6-morpholin-4-yl-9H-purine, PDB code ZYU [26]. Docking validation was performed by calculating the binding modes (between ZYU and Chk1) in the Autodock 4.2.6 program [27], using the standard genetic algorithm parameters, with population size 150, maximum number of Ratings 250000, maximum number of generations 27000 and crossover rate 0.8. The values for the dimensions of the grid box were: X = 25, Y = 30 and Z = 20 and the center location was x = 12.6747, y = -2.0751 and z = 7.9635. Ten solutions were calculated and the poses with lower binding energies were analyzed.

Docking validation is a process wherein a ligand (structure with crystallographic pose experimentally determined) is withdrawn from the structure of a receptor-ligand complex, and reintroduced to the receptor with the docking parameters to be validated. This process is conducted in order to verify that the coupling parameters specified in the input file for the docking method are reasonable and able to recover the structure and interactions of a known complex [27].

The best molecules obtained from pharmacokinetic and toxicological screening, caffeine and molecule 03 (the last two used as reference) were submitted to molecular docking using the same standard genetic algorithm parameters used in docking validation. The center location and grid box dimensions were also used as spatial orientation of the site of interaction between the ligand and the Chk1 receptor.

3. RESULTS and DISCUSSIONS

3.1. Pharmacophore Generation

The best model was chosen according to the pharmacophore candidate containing the highest score as well as the multiple alignment of the 21 ligands of the training set. PharmaGist generates pharmacological candidate scores based on the alignment of the ligands with the pivot molecule (here treated as reference and keeped rigid). The server algorithm uses values with standard weights for each pharmacophoric characteristic. Initially, the alignment of the pivot + ligand pair is scored by their common characteristics and then the multiple alignment between the best scored pairs is generated. Various multiple alignments are thus scored by the same way [16, 17].

The quantitative characteristics of the best model are shown in Table **1**, and the qualitative ones are shown in Figure **2**.

Table 1. Data found on the best PharmaGist pharmacophore model.

Score	GF	SF	Ar	Hyd	Don	Acc	Neg	Pos	Molecules in multiple alignment
60.852	6	6	2	0	0	3	0	1	01*, 02, 03, 04, 05, 06, 07, 08, 09, 10, 11, 12, 13, 14, 15, 16, 17, 18, 19, 20, 21.

A = number of atoms; GF = General Characteristics; SF = Spatial Characteristics; Ar = Aromatic; Hyd = Hydrophobic; Don = Hydrogen bond donor; Acc = Hydrogen bond acceptor; Neg = Anion; Pos = Cation.

*Pivot molecule (Caffeine).

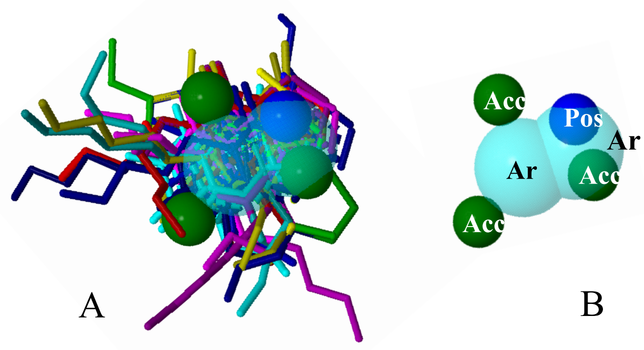

Fig. (2). Qualitative characteristics of the best model generated by PharmaGist, with aligned ligands (**A**) and no aligned ligands (**B**).

The model shows six general characteristics (GF), which represent the total pharmacophoric characteristics; six spatial characteristics (SF) related to the conformation of pharmacophoric regions; two aromatic regions (Ar); three hydrogen bond acceptor goups (Acc) and 1 cationic atom (Pos).

The training set consisted of the most active molecules, caffeine and xanthine. The structures and names of the molecules selected for the training set can be seen in Fig. **3**.

The pharmacophoric data, the values of ICT_{50} and $pICT_{50}$, and the their best correlations between with the variables of the 21 molecules of the training set are shown in Table **2**. These data describe the individual pharmacophoric characteristics with significant correlations to the experimental activity values.

Properties with absolute correlation values less than 0.3 and greater than - 0.3 were excluded. The best correlations were related to the pharmacophoric properties A, GF, SF, Hyd, with positive correlations between them greater than 0.9. The correlation values between the properties and $pICT_{50}$ were also significant, all between 0.7 and 0.8. These results are considered of good statistical quality for the selection of more significant characteristics [18, 28].

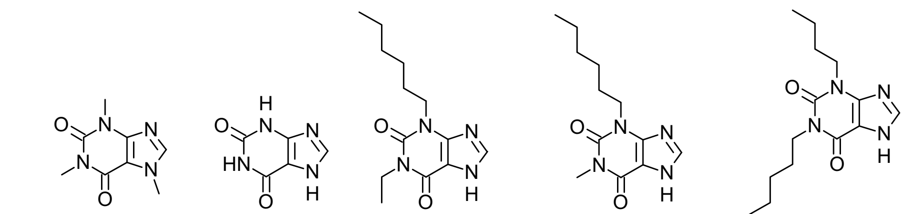

(01) 1,3,7-trimethylxanthine (Caffeine)
(02) xanthine
(03) 1-ethyl-3-hexylxanthine
(04) 3-hexyl-1-methylxanthine
(05) 3-butyl-1-pentylxanthine

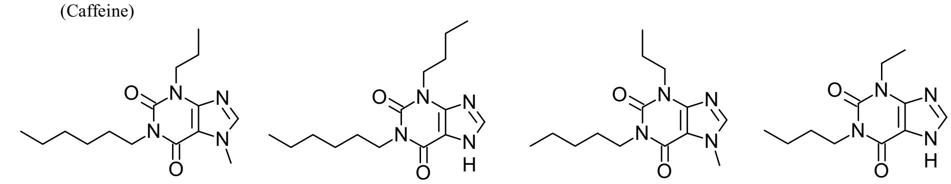

(06) 1-hexyl-7-methyl-3-propylxanthine
(07) 3-butyl-1-hexylxanthine
(08) 7-methyl-1-pentyl-3-propylxanthine
(09) 1-butyl-3-ethylxanthine

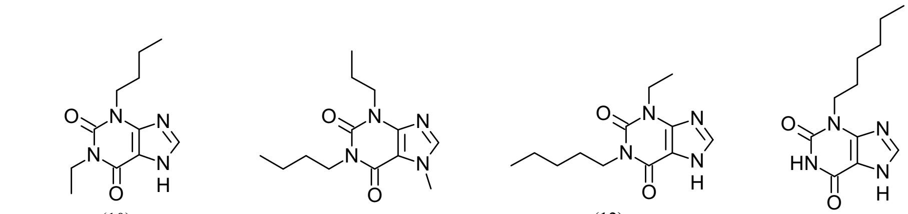

(10) 3-butyl-1-etylxanthine
(11) 1-butyl-7-methyl-3-propylxanthine
(12) 3-ethyl-1-pentylxanthine
(13) 3-hexylxanthine

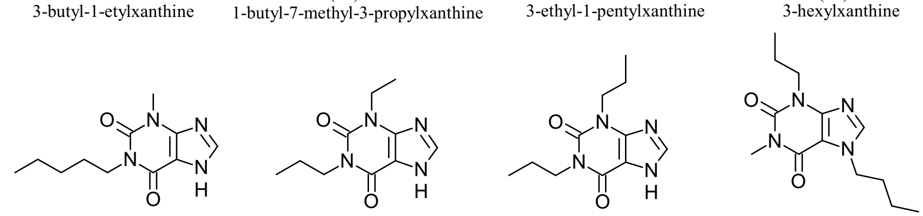

(14) 3-methyl-1-pentylxanthine
(15) 3-ethyl-1-propylxanthine
(16) 1,3-dipropylxanthine
(17) 7-butyl-1-methyl-3-propylxanthine

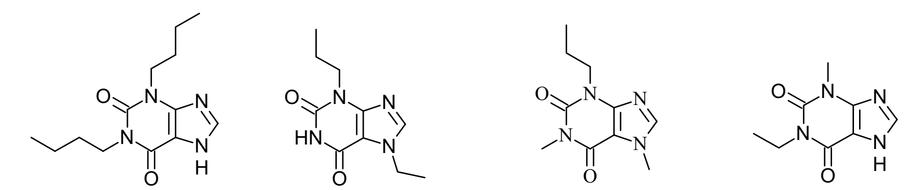

(18) 1,3-dibutylxanthine
(19) 7-ethyl-3-propylxanthine
(20) 1,7-dimethyl-3-propylxanthine
(21) 1-ethyl-3-methylxanthine

Fig. (3). Molecules of the training set used for pharmacophore generation.

3.1.1. Construction of MLR models

MLR models were built with the four best correlated pharmacophoric properties. The evaluation of the best models was carried out from the statistical descriptors of correlation coefficient (R), coefficient of determination (R^2), adjusted coefficient of determination (R_A^2), Standard Error of Estimation (SEE), analysis of variance and T test, which can be seen in Table **3**.

3.2. MLR Models and Validation

Data from the best MLR models resulting from combinations of one, two, three and four parameters are in bold. The values of R, R^2 and R_A^2 increased with the increase in the number of parameters of the models, the highest values were found in tetra-parametric model and the smaller values in the mono-parametric model. The values of SEE decreased with increasing number of parameters, the tetra-parametric model presented the lowest value and the mono-parametric the highest.

The values of F decreased with increasing number of parameters. The results of the t-test for the regression coefficients (Table **4**) indicate that the parameters A and GF in the tetra and tri-parametric models presented significant values, as well as the GF parameter in the bi and mono-parametric models. The results for R, R^2, R_A^2, SEE and t-test, lead us to define, even with the low significance shown by the values of F, that the four models highlighted have a good level of statistical significance, being the tetra-parametric model the best classified.

The regression equations for each of the best models (shown in bold, in Table **3**) are shown in Table **5**.

3.2.1. Internal and external validation of MLR models

The equations proposed in Table **5** were used to predict the activity of the training set molecules (internal validation), the test set (external validation) and the selected molecules. The results for the $pICT_{50}$ values calculated for each molecule of the training set from the regression equations are available in Table **6**.

Table 2. Pharmacophoric Characteristics of the Training set, $pICT_{50}$ and ICT_{50} values, and correlation between the most Significant properties.

Training Set Molecules	A	GF	SF	Ar	$pICT_{50}$	ICT_{50}
1 (caffeine)	24	9	9	0	0.3188	0.48
2 (xantine)	15	9	8	3	0.3468	0.45
3	39	13	12	6	2.0000	0.01
4	36	13	12	6	1.6990	0.02
5	42	14	13	7	1.5229	0.03
6	45	14	14	8	1.5229	0.03
7	45	15	14	8	1.5229	0.03
8	42	13	13	7	1.3979	0.04
9	33	11	10	4	1.3010	0.05
10	33	11	10	4	1.3010	0.05
11	39	12	12	12	1.3010	0.05
12	36	12	11	11	1.3010	0.05
13	33	13	12	12	1.3010	0.05
14	33	12	11	11	1.0000	0.10
15	30	10	9	9	0.9208	0.12
16	33	11	10	10	0.8861	0.13
17	39	12	12	12	0.8861	0.13
18	39	13	12	12	0.8239	0.15
19	30	10	10	10	0.7959	0.16
20	30	10	10	10	0.6990	0.20
21	24	9	8	8	0.6198	0.24
	A	GF	SF	Hyd	$pICT_{50}$	
A	1.000000	0.904527	0.934078	0.974591	0.767452	-
GF		1.000000	0.962751	0.933680	0.800355	-
SF			1.000000	0.960847	0.738313	-
Hyd				1.000000	0.747840	-
$pICT_{50}$					1.000000	-

The results of Table **6** allow us to observe that the models had a good predictability level for the training set molecules, since the error values (Δ - variation of the experimental $pICT_{50}$ values), in general, were relatively low for all models. The tetra-parametric model should be emphasized when considering the Δ4 modules, which presented a mean error of 0.1662 and a minimum and maximum interval of 0.0030 to 0.4800, lower results for this series of data among all the models.

Fig. **4** shows the correlation between the calculated experimental $pICT_{50}$ and calculated $pICT_{50}$ for each model. The models presented good correlation indexes, with R values around 0.8. The analysis of Fig. **4** also shows good results of the tetra-parametric model, where it has the highest value of R (0.85872), with an excellent confidence level, against a value of R = 0.80037 of the monoparametric model. Table **7** shows the pharmacophoric data, the ICT_{50} and $pICT_{50}$ values of the 9 molecules (22 to 30) of the test set. Figure 5 shows the structures of the test set molecules. Data on the $pICT_{50}$ calculations for the test set are presented in Table **8**. These calculations were performed from the best MLR models, similar to those performed for the training set.

The results of Table **8** show that the prediction using the models on the test set was satisfactory. The mono and tetra-parametric models showed mean error of 0.2150 and 0.3381, respectively. Fig. **6** shows the correlation between the calculated and experimental $pICT_{50}$ values in each model. The four models presented excellent R values, all of them above 0.9,, at the 95% confidence level.

Table 3. Statistical data of MLR models generated from the pharmacophoric characteristics of the training set in respect to $pICT_{50}$ values.

Mono-parametric Models						
Eq.	**Descriptor**	**R**	**R^2**	**R^2_A**	**SEE**	**F**
1	**GF**	**0.8004**	**0.6406**	**0.6217**	**0.2703**	**33.8612**
2	A	0.7675	0.5890	0.5674	0.2890	27.2268
3	SF	0.7383	0.5451	0.5212	0.3040	22.7680
4	Ar	0.0876	0.0076	-0.0445	0.4491	0.1470
Di-parametric Models						
Eq.	Descriptor	R	R^2	R^2_A	SEE	F
1	**GF +Ar**	**0.8177**	**0.6686**	**0.6317**	**0.2666**	**18.1548**
2	GF + SF	0.8092	0.6548	0.6164	0.2721	17.0700
3	A + GF	0.8068	0.6510	0.6122	0.2737	16.7865
4	A + Ar	0.7990	0.6384	0.5982	0.2786	15.8859
5	A + SF	0.7698	0.5926	0.5473	0.2956	13.0909
6	SF + Ar	0.7559	0.5714	0.5238	0.3032	11.9987
Tri-parametric Models						
Eq.	Descriptor	R	R^2	R^2_A	SEE	F
1	**A + GF + SF**	**0.8336**	**0.6949**	**0.6410**	**0.2632**	**12.9045**
2	A + GF + Ar	0.8312	0.6909	0.6363	0.2650	12.6643
3	GF + SF + Ar	0.8238	0.6787	0.6220	0.2701	11.9706
4	A + SF + Ar	0.7999	0.6399	0.5764	0.2859	10.0714
Tetra-parametric Model						
Eq.	Descriptor	R	R^2	R^2_A	SEE	F
1	**A + SF + GF + Ar**	**0.8587**	**0.7374**	**0.6717**	**0.2517**	**11.2318**

Table 4. Results of the t test for the regression coefficients of the best models.

Model	**Variable**	**t-test**	**p Value**
Tetra-parametric A + SF + GF + Hyd	Intercept	-0.9925	0.3357
	A	1.1138	0.2818
	GF	2.2835	0.0364
	SF	-0.9999	0.3323
	Hyd	-0.2890	0.7763
Tri-parametric A+GF+SF	Intercept	-2.1310	0.4880
	A	1.4945	0.1534
	GF	2.3871	0.0289
	SF	-1.5637	0.1363

(Table 4) Contd....

Model	Variable	t-test	p Value
Bi-parametric GF+Hyd	Intercept	-1.5580	0.1366
	GF	2.0179	0.0588
	Hyd	0.0112	0.9912
Mono-parametric GF	Intercept	-3.0010	0.0073
	GF	5.8190	0.000013

Table 5. Regression equations for the best models.

Model (Eq.) (n = 21)	Equation
Mono-parametric (Eq1)	$pICT_{50} = -1.2168(\pm0.4055) + 0.1993(\pm0.0342) \times GF$
Bi-parametric (Eq2)	$pICT_{50} = -1.888(\pm0.4007) + 0.2128(\pm0.0355) \times GF - 0.0230(\pm0.0187) \times Hyd$
Tri-parametric (Eq3)	$pICT_{50} = -0.9477(\pm0.4447) + 0.0334(\pm0.0224) \times A + 0.2949(\pm0.1235) \times GF - 0.2295(\pm0.1468) \times SF$
Tetra-parametric (Eq4)	$pICT_{50} = -0.8324(\pm0.4312) + 0.0415(\pm0.0220) \times A + 0.2881(\pm0.1182) \times GF - 0.2364(\pm0.1404) \times SF - 0.0293(\pm0.0182) \times Hyd$

Table 6. Prediction of $pICT_{50}$ values of MLR models (equations 1 to 4) applied to the training set, experimental $pICT_{50}$ values, mean error and maximum and minimum values

Training set	Mono-parametric		Bi-parametric		Tri-parametric		Tetra-parametric		
	Eq1	Δ1	Eq2	Δ2	Eq3	Δ3	Eq4	Δ4	$pICT_{50}$
1 (Caffeine)	0.5766	-0.2578	0.7262	-0.4074	0.4432	-0.1244	0.6297	-0.3109	0.3188
2	0.5766	-0.2298	0.6572	-0.3104	0.3719	-0.0251	0.4043	-0.0575	0.3468
3	1.3737	0.6263	1.4393	0.5607	1.4357	0.5643	1.5200	0.4800	2.0000
4	1.3737	0.3253	1.4393	0.2597	1.3354	0.3636	1.3954	0.3036	1.6990
5	1.5730	-0.0501	1.6290	-0.1061	1.6014	-0.0785	1.6670	-0.1441	1.5229
6	1.5730	-0.0501	1.6060	-0.0831	1.4721	0.0508	1.5259	-0.0030	1.5229
7	1.7722	-0.2493	1.8188	-0.2959	1.7670	-0.2441	1.8140	-0.2911	1.5229
8	1.3737	0.0242	1.4163	-0.0184	1.3065	0.0914	1.3790	0.0189	1.3979
9	0.9752	0.3258	1.0597	0.2413	1.1043	0.1967	1.2260	0.0750	1.3010
10	0.9752	0.3258	1.0597	0.2413	1.1043	0.1967	1.2260	0.0750	1.3010
11	1.1744	0.1266	1.0885	0.2125	1.1408	0.1602	1.0561	0.2449	1.3010
12	1.1744	0.1266	1.1115	0.1895	1.2700	0.0310	1.1971	0.1039	1.3010
13	1.3737	-0.0727	1.3013	-0.0003	1.2352	0.0658	1.0949	0.2061	1.3010
14	1.1744	-0.1744	1.1115	-0.1115	1.1697	-0.1697	1.0725	-0.0725	1.0000
15	0.7759	0.1449	0.7320	0.1888	0.9386	-0.0178	0.9032	0.0176	0.9208
16	0.9752	-0.0891	0.9217	-0.0356	1.1043	-0.2182	1.0501	-0.1640	0.8861
17	1.1744	-0.2883	1.0885	-0.2024	1.1408	-0.2547	1.0561	-0.1700	0.8861
18	1.3737	-0.5498	1.3013	-0.4774	1.4357	-0.6118	1.3441	-0.5202	0.8239

(Table 6) Contd....

Training set	Mono-parametric		Bi-parametric		Tri-parametric		Tetra-parametric		
	Eq1	Δ1	Eq2	Δ2	Eq3	Δ3	Eq4	Δ4	$pICT_{50}$
19	0.7759	0.0200	0.7090	0.0869	0.7091	0.0868	0.6375	0.1584	0.7959
20	0.7759	-0.0769	0.7090	-0.0100	0.7091	-0.0101	0.6375	0.0615	0.6990
21	0.5766	0.0432	0.5422	0.0776	0.6727	-0.0529	0.6315	-0.0117	0.6198
*Mean error		0.1989		0.1960		0.1704		0.1662	
*Max		0.6263		0.5607		0.6118		0.4800	
*Min		0.0200		0.0003		0.0101		0.0030	

* The module of the error values was considered for this determination.

Table 7. Pharmacophoric characteristics of test set, $pICT_{50}$ and ICT_{50} values.

Test set	A	GF	SF	Hyd	$pICT_{50}$	ICT_{50}
22	39	13	12	6	1.3010	0.05
23	30	11	10	4	0.7447	0.18
24	33	10	10	4	0.6021	0.25
25	33	10	10	4	0.5229	0.30
26	27	9	8	2	0.4202	0.38
27	18	9	8	1	0.3279	0.47
28	21	9	9	2	0.3279	0.47
29	21	9	8	1	0.3098	0.49
30	21	9	8	1	0.2924	0.51

Table 8. Prediction of the $pICT_{50}$ values for the MLR models (equations 1 to 4) in respect to the training set, experimental $pICT_{50}$ values, mean error and maximum and minimum values.

	Mono-parametric		Bi-parametric		Tri-parametric		Tetra-parametric		
Structure	Eq1	Δ1	Eq2	Δ2	Eq3	Δ3	Eq4	Δ4	$pICT_{50}$
22	1.3738	-0.0727	1.4393	-0.1382	1.4357	-0.1347	1.5209	-0.2199	1.3010
23	0.9752	-0.2305	1.0597	-0.3150	1.0041	-0.2593	1.1020	-0.3573	0.7447
24	0.7759	-0.1739	0.8469	-0.2449	0.8094	-0.2073	0.9386	-0.3365	0.6021
25	0.7759	-0.2531	0.8469	-0.3241	0.8094	-0.2865	0.9386	-0.4157	0.5229
26	0.5767	-0.1565	0.6802	-0.2600	0.7729	-0.3527	0.9324	-0.5121	0.4202
27	0.5767	-0.2488	0.7032	-0.3753	0.4722	-0.1443	0.5877	-0.2598	0.3279
28	0.5767	-0.2488	0.6802	-0.3523	0.3429	-0.0150	0.4467	-0.1188	0.3279
29	0.5767	-0.2669	0.7032	-0.3934	0.5724	-0.2626	0.7123	-0.4025	0.3098
30	0.5767	-0.2842	0.7032	-0.4107	0.5724	-0.2800	0.7123	-0.4199	0.2924
*Mean error		0.2150		0.3127		0.2158		0.3380	
*Max		0.2842		0.4107		0.3527		0.5121	
*Min		0.0727		0.1382		0.0150		0.1188	

* The module of the error values was considered for this determination.

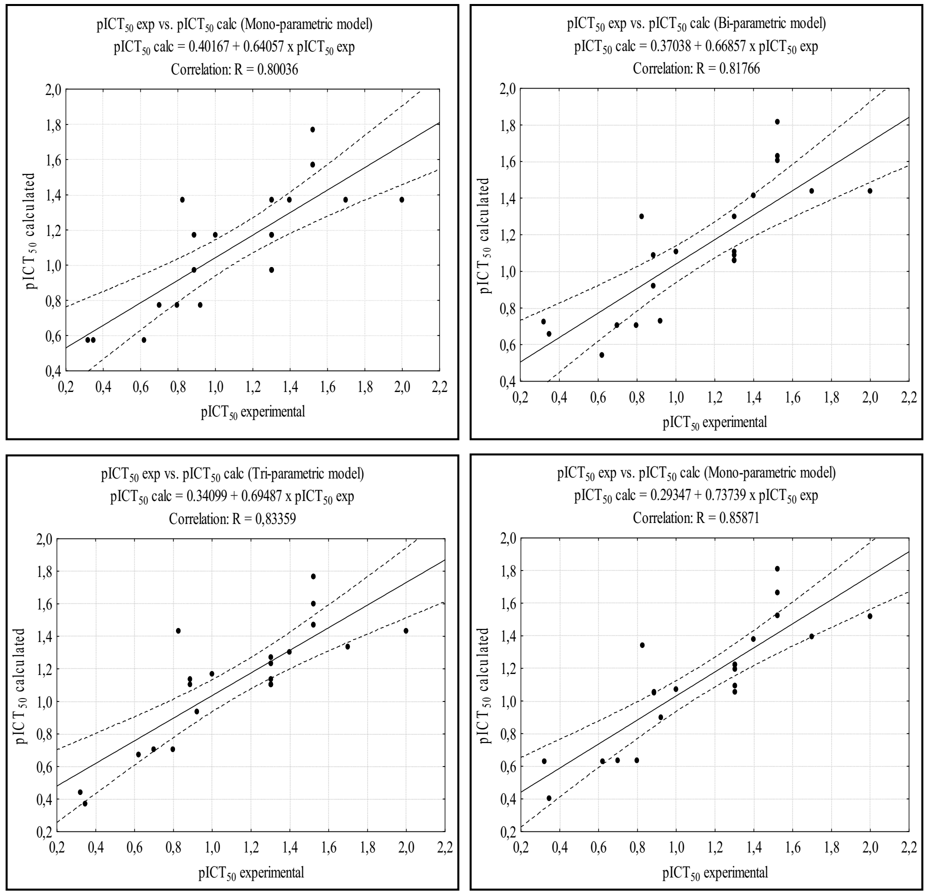

Fig. (4). Correlation between the calculated and experimental $pICT_{50}$ values of the training set are shown. The dashed lines near to the center line represent the confidence interval (95%).

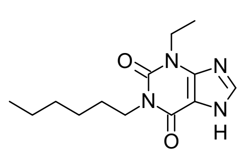

(22)
3-etyl-1-hexylxanthine

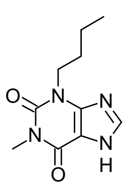

(23)
3-butyl-1-methylxanthine

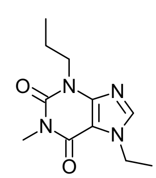

(24)
7-etyl-1-methyl-3-propilxanthine

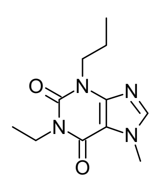

(25)
1-etyl-7-methyl-3-propylxanthine

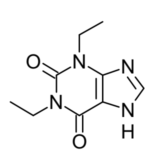

(26)
1,3-dietylxanthine

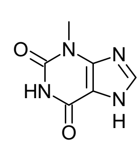

(27)
3-methylxanthine

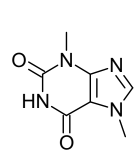

(28)
3,7-dimethylxanthine

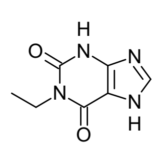

(29)
1-etylxanthine

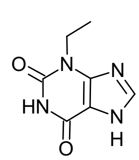

(30)
3-ethylxanthine

Fig. (5). Molecules of the test set.

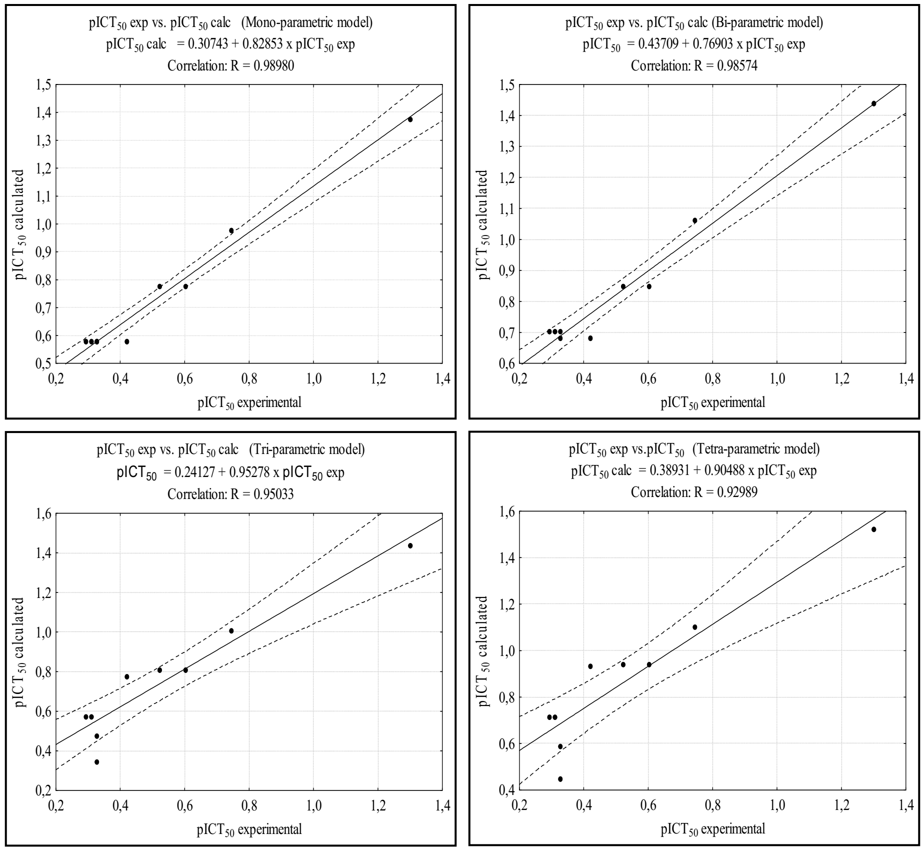

Fig. (6). Correlation between the calculated and experimental $pICT_{50}$ values of the test set. The dashed lines near to the center line represent the confidence interval (95%).

The tetra-parametric model can be considered the most reliable of the models, regarding the prediction of $pICT_{50}$ values, also due to statistical consistencies observed from the regression data (R, R^2, R_A^2, SEE e teste t) discussed above. The statistically significant values presented provide confidence to the MLR models and their predictive capacity [29, 30].

3.3. Selection from the ZINC Database

Pharmacophore-based screening performed on ZINCPharmer web server resulted in 350 ZINC molecules. Such tool selects the molecules according to the characteristics of the inserted pharmacophore. One of the main filters of this tool is the root mean square deviation (RMSD) estimation calculated between the characteristics of the input file (pharmacophile model) and the resulting molecules, as well as other filters such as molecular weight and rotational bonds [28].

3.3.1. Similarity of Tanimoto and Estimation of $pICT_{50}$ Values for ZINC Molecules

The pharmacophore data and the $pICT_{50}$ values calculated for the ZINC molecules with the best Tanimoto indices can be seen in Table **9**. The BindingDB server was used to select, from the 350 ZINC molecules screened in the previous step, the ones with values of maximum similarity greater than 0.6, which resulted in 24 molecules (Table **9**).

The bindingDB web server performs similarity search as a function of chemical fingerprints (a kind of set of chemical characteristics treated as chemical fingerprints) that characterize the molecules [31, 32].

Chemical fingerprints are used in conjunction with Tanimoto's similarity by comparing each selected molecule with each molecule in the reference set and ordering the molecules in function of maximum similarity to any active molecule in the reference set [31-33]. The closer to 1 the values are, the greater the degree of similarity of the molecules to the molecules indicated as a reference.

The structures of the 24 ZINC molecules sorted out can be seen in Fig. **7**.

3.4. Prediction of Pharmacokinetic and Toxicological Properties

At this stage, the selection of the best molecules was based on the best pharmacokinetic and toxicological properties. The higher the values for the human intestinal absorption rate and Plasma Protein Binding, the more efficient the drug is in respect to each of these pharmacokinetic properties. However, for blood-brain barrier, Mutagenicity and Carcinogenicity, low values are desirable.

The predictions of pharmacokinetic and toxicological properties (Table **10**) were performed for the molecules selected by Tanimoto's similarity, located within the cut-off point having as reference molecules 3-7 (only molecules with $pICT_{50} > 1.5229$ were selected). The use of the cut-off point resulted in the selection of the 10 most active molecules (Table **10**). The caffeine molecule and molecule 03 (most active) from the training set were inserted into Table **10** as reference values.

The prediction of human intestinal absorption (HIA) is measured as a function of the absorption fraction, %HIA, described as the percentage of the dose of the drug administered orally to reach the hepatic portal vein. It is also defined as the rate of total absorbed mass divided by the dose of the drug. This property is used to assess the degree of absorption of a drug, orally administered, by the intestinal epithelium [34].

Absorption levels below 25% are considered poor and greater than 80% are considered high. The results of HIA were considered excellent since, for all the sorted molecules, HIA values were

Table 9. Pharmacophore characteristics and $pICT_{50}$ values calculated for the sorted molecules.

ZINC Molecules Selected	Pharmacophoric Characteristics				Tanimoto Index	Calculated $pICT_{50}$			
	A	GF	SF	Hyd		Eq1	Eq2	Eq3	Eq4
ZINC08791938	34	13	13	5	0.67	1.3738	1.4623	1.0391	1.1053
ZINC08990240	42	16	16	8	0.71	1.9716	2.0316	1.5027	1.5047
ZINC08992920	37	14	14	6	0.66	1.5730	1.6520	1.2048	1.2522
ZINC09060391	43	13	13	4	0.71	1.3738	1.4853	1.3399	1.5084
ZINC10104345	42	15	15	7	0.77	1.7723	1.8418	1.4373	1.4823
ZINC10104354	36	13	13	5	0.70	1.3738	1.4623	1.1059	1.1883
ZINC10104357	39	14	14	6	0.73	1.5730	1.6520	1.2716	1.3353
ZINC10233741	30	11	11	3	0.68	0.9752	1.0827	0.7746	0.8944
ZINC10233742	39	14	14	6	0.76	1.5730	1.6520	1.2716	1.3353
ZINC10233743	31	11	11	3	0.65	0.9752	1.0827	0.8080	0.9359
ZINC10233744	40	13	13	4	0.61	1.3738	1.4853	1.2396	1.3838
ZINC10233745	40	13	13	4	0.61	1.3738	1.4853	1.2396	1.3838
ZINC10233747	33	12	12	4	0.67	1.1745	1.2725	0.9403	1.0414
ZINC10233748	34	12	12	4	0.64	1.1745	1.2725	0.9737	1.0829
ZINC08706084	36	14	14	6	0.70	1.5730	1.6520	1.1714	1.2107
ZINC08706127	39	15	15	7	0.73	1.7723	1.8418	1.3371	1.3577
ZINC08706179	41	13	13	4	0.61	1.3738	1.4853	1.2730	1.4254
ZINC08706191	37	14	14	6	0.62	1.5730	1.6520	1.2048	1.2522
ZINC08706200	37	11	11	2	0.62	0.9752	1.1057	1.0085	1.2145
ZINC08706215	40	12	12	3	0.61	1.1745	1.2955	1.1742	1.3615
ZINC08709887	43	14	14	5	0.61	1.5730	1.6750	1.4053	1.5308
ZINC08710197	36	13	13	5	0.75	1.3738	1.4623	1.1059	1.1883
ZINC08724916	37	11	11	2	0.61	0.9752	1.1057	1.0085	1.2145
ZINC08725388	43	14	14	5	0.61	1.5730	1.6750	1.4053	1.5308

higher than the two reference values (caffeine = 93.82% and molecule 03 = 88.13%) and close to 100%. These values attribute high-grade intestinal absorption to the ZINC molecules.

Plasma protein binding property (PPB) is defined as the percentage of a drug bound to plasma proteins at clinically achieved concentrations of the drug. PPB is important for evaluating the performance of a drug in the bioavailable free fraction distributed across several tissues [35]. Values of PPB above 65% are considered of high clinical significance and lower values are of low significance [36-38].

The molecules ZINC08709887 and ZINC08725388 showed higher PPB values (89.15% and 94.19%, respectively), values higher than that of the molecule 03 used as reference. All the triad molecules presented PPB values (range, 50.13% to 94.19%) higher than that of caffeine (14.07%), showing satisfactory results when compared to this reference.

Experimental PPB results for caffeine, available in the literature, show values of 35% [39], 36% [40] and 40% [41]. These values show an average error of 22.93% in respect to the PPB value of caffeine calculated by Preadmet. The margin of error of 22.93% applied to the chosen molecules theoretically allows the framing of part of this set of molecules between the clinically relevant PPB values (above 65%).

The blood-brain barrier is a specialized structure that has a protective function of the Central Nervous System (CNS). This barrier controls and regulates the homeostasis of the central nervous system through the separation of brain (C_{brain}) and systemic blood (C_{blood}). For a drug with biological activity in the CNS, a high penetration value is required. However, for a drug without CNS activity, as herein investigated, low penetration value is required, so that side effects are minimized [35, 42].

For the ZINC molecules the values of BBB were all lower than the value presented by molecule 03 (<1.60), see Table **10**. According to the literature [43], BBB values less than 1 (C_{brain} / C_{blood} <1)

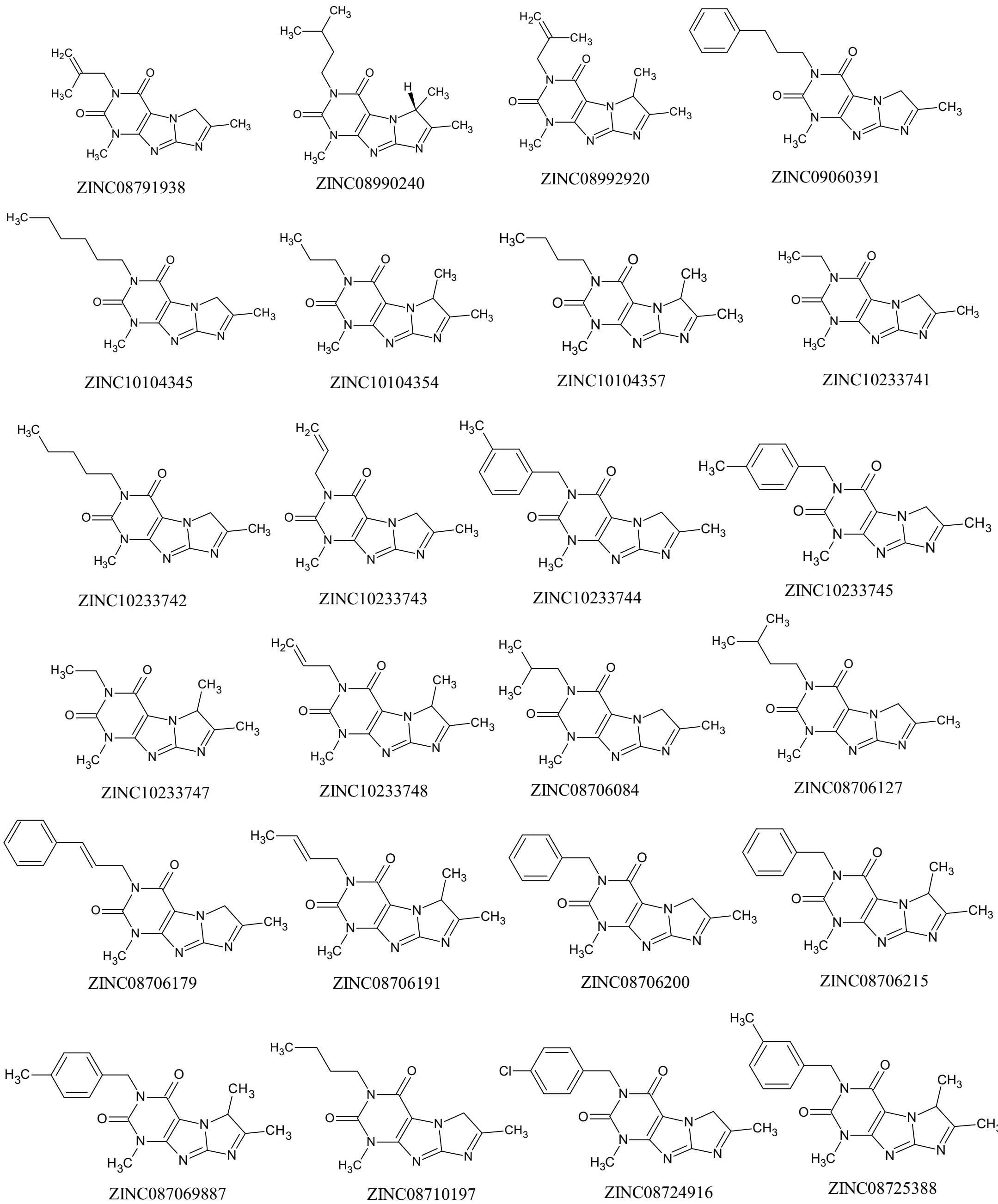

Fig. (7). Structure of the ZINC molecules selected by the Tanimoto index.

give the molecule an inactive status in the CNS. This means that only the molecule ZINC08990240 (BBB = 1.09) and molecule 03 (BBB = 1.60) showed penetration into the CNS, which qualifies the majority of ZINC molecules as inactive in the CNS.

The results for the pharmacokinetic parameters found for caffeine and ZINC molecules, are consistent with the findings of Liu, Shen, Shi and Cai (2016) [44], In their study, the authors concluded that caffeine is directly related to the reduction of the risk of malignant melanoma. Through meta-analysis, the authors identified a low relative risk of malignant melanoma related to high consumption of caffeinated coffee, suggesting that caffeine present in caffeinated coffee has a chemopreventive effect against malignant melanoma. Unlike decaffeinated coffee that showed no significant relationship with the risk of malignant melanoma.

The toxicological properties, shown in Table **10**, were predicted by the Ames test (mutagenicity) and carcinogenicity test. The Ames test consists of an assay that aims the mutagenic reversal of bacteria (Salmonella typhimurium) tested for histidine independence. Preadmet simulates tests for strains TA100 and TA1535, which serve to evaluate the mutagenic potential of molecules, ie the ability to generate mutation in an organism. This test simulates an environment in which a post-mitochondrial mouse liver supernatant mixture treated with a mixture of phenobarbital / β-naphthoflavone (s9) may be present or absent [45, 46]. The in silico carcinogenicity test simulates the presence of the drug in the organism of rats and mice, and it is possible to evaluate if the drug has the power to generate tumors [47].

Table 10. Prediction of pharmacokinetic and toxicological properties of molecules with better $pICT_{50}$ values

Molecules	Pharmacokinetic Parameters			Toxicological Parameters		
	HIA (%)	PPB (%)	BBB (C.brain/C.blood)	Mutagenicity	Carcinogenicity	
				Result	Rat	Mouse
Caffeine	93.82	14.07	0.33	Mutagenic	Positive	Negative
Molecule 03	88.13	75.91	1.60	Mutagenic	Negative	Negative
ZINC08706084	96.27	50.13	0.59	Mutagenic	Negative	Negative
ZINC08706127	96.89	55.18	0.75	Mutagenic	Negative	Negative
ZINC08706191	97.53	64.25	0.65	Mutagenic	Positive	Positive
ZINC08709887	98.83	89.15	0.47	Mutagenic	Negative	Negative
ZINC08725388	98.83	94.19	0.28	Mutagenic	Negative	Negative
ZINC08990240	97.41	63.51	1.09	Mutagenic	Negative	Negative
ZINC08992920	97.53	63.15	0.80	Mutagenic	Positive	Negative
ZINC10104345	97.41	74.20	0.18	Mutagenic	Negative	Negative
ZINC10104357	96.89	60.59	0.90	Mutagenic	Negative	Negative
ZINC10233742	96.89	68.86	0.15	Mutagenic	Negative	Negative

HIA = Human Intestinal Absorption; **PPB** = Plasma Protein Binding; **BBB** = Blood-Brain Barrier Penetration

Regarding the results for mutagenicity in Preadmet software, all screened and reference molecules were classified as mutagenic. Even showing mutagenicity, where elimination of molecules for this reason would be premature, studies with rats have shown that a mutagenic molecule when administered in combination with an antimutagenic (chemopreventive) agent may cause suppression of the mutagenic action [48, 49].

For carcinogenicity in Preadmet softtware, caffeine and the molecule ZINC08992920 showed positive results (non-carcinogenic) in rats and negative (carcinogenic) results in mice. Only the molecule ZINC08706191 presented positive results, both for mouse and rat, which allows to classify it with non-carcinogenic in Preadmet softtware.

Additional data on toxicological parameters for caffeine, molecule 03 and ZINC molecules tested in the Derek program [23] can be seen in Table **11**.

Data of Table **11** indicate that both reference molecules (caffeine and molecule 03) showed teratogenicity, representing the possibility of a substance causing abnormal formation during the gestation period. Only caffeine presented a possibility of chromosome damage, which represents the ability to generate changes in the molecular structure of the chromosome. The Derek software identified the reference scaffold/moety of xanthine present in caffeine and molecule 03 as part of the structure of the molecules responsible for the teratogenic and chromosome damage effects. None of the ZINC molecules tested showed potential for teratogenic and chromosome damage. These results allow to classify the ZINC molecules as better than the reference molecules in respect to the two toxicological parameters mentioned.

However, nine of the ten ZINC molecules tested showed toxicity to skin sensitization. This effect corresponds to an allergic response after contact of a substance with the skin [50]. This sensitization was attributed by the Derek program to the imine toxicoforic group, being able to occur nucleophilic attack of skin proteins to the carbon atom of the imine group [51].

Unlike the results presented for tests of mutagenicity and carcinogenicity carried out in Preadmet, all molecules were excluded from the mutagenicity and carcinogenicity alert in the Derek software, no toxicological groups are identified that could indicate such toxicological parameters.

With respect to chromosome damage and mutagenicity, a review on caffeine [52], showed that chromosome damage data from studies with caffeine were obtained at concentrations of about 6 to 100 times higher than expected for frequent coffee users and with magnitude above the lethal dose of caffeine in humans. Such as most non-mutagenic substances in *in vitro* tests, they are non-carcinogenic in mammals, it is unlikely that at the usual consumption level caffeine presents any mutagenic and carcinogenic risk. Such dose-effect dependency of caffeine on mutagenicity was also evidenced in a study on the mutagenic action of caffeine in higher organisms [53]. It is possible to infer from these studies that mutagenicity (existing for all ZINC molecules tested in Preadmet) has a strong dose-effect relationship when it comes to caffeine. In this context, the results of Preadmet and Derek obtained for the tested molecules can be interpreted as a possibility of toxicity depending on the level of consumption or the dose administered, which suggests that mutagenicity for the most promising molecules should be more thoroughly investigated in *in vitro* and *in vivo* analyzes, and not taken as conclusive.

Still in Table **11** it is possible to verify the hits related to the toxicity of each molecule. Such as the caffeine that has been shown to be mutagenic and carcinogenic in mice (Preadmet), besides teratogenic and promoter of chromosome damage (Derek), 4 hits of toxicity are predicted. Since the higher the hit value the greater the toxicity, the molecules ZINC08992920 (3 hits) and ZINC08706191 (1 hit and no toxicity alert on Derek) as less toxic in comparison to the other molecules (all with 4 hits). The molecule ZINC08706191 is the best one qualified in respect to toxicity, because there is no carcinogenic risk in both Preadmet and Derek softwares.

Table 11. Toxicity results obtained using the Derek software.

Molecule	Toxicity Prediction Alert (Lhasa prediction)	Toxicophoric Group	Toxicity Alert	Hits*
Caffeine	Chromosome damage	Xhantine	Certain	4
	Teratogenicity	Xhantine	Probable	
Molecule 03	Teratogenicity	Xhantine	Plausible	4
ZINC08706084	Skin sensitisation	Imine or alpha,beta-unsaturated imine	Plausible	4
ZINC08706127	Skin sensitisation	Imine or alpha,beta-unsaturated imine	Plausible	4
ZINC08706191	No Alerts	—	No Alerts	1
ZINC08709887	Skin sensitisation	Imine or alpha,beta-unsaturated imine	Plausible	4
ZINC08725388	Skin sensitisation	Imine or alpha,beta-unsaturated imine	Plausible	4
ZINC08990240	Skin sensitisation	Imine or alpha,beta-unsaturated imine	Plausible	4
ZINC08992920	Skin sensitisation	Imine or alpha,beta-unsaturated imine	Plausible	3
ZINC10104345	Skin sensitisation	Imine or alpha,beta-unsaturated imine	Plausible	4
ZINC10104357	Skin sensitisation	Imine or alpha,beta-unsaturated imine	Plausible	4
ZINC10233742	Skin sensitisation	Imine or alpha,beta-unsaturated imine	Plausible	4

* Sum of hits corresponding to the toxicological analyzes performed in Preadmet and Derek.

3.5. Molecular Docking

Molecular docking allows the collection of data on interactions between ligand and receptor, making possible the selection of the best ligand poses as a function of the lowest free energy which results from that interaction. For the molecular docking step only the molecules ZINC08706191 (1 hit of toxicity) and ZINC08992920 (3 hit of toxicity), classified as less toxic, were selected.

3.5.1. Receptor-ligand Complex

Selection of the receptor-ligand complex Chk1 was performed initially by taking into account the structure of the ligand compared to the xanthine scaffold and size of the ligands (smaller molecules), which resulted in 6 molecules (Fig. **8**).

The results for overlap similarity between the selected binders and caffeine can be seen in Table **12**. Values for overlap similarity attributed to 100% estrogenic contribution (100ste), 100% electrostatic contribution (100elt), 60% steric and 40% electrostatic (60ste/40elt), 40% steric and 60% electrostatic (40ste / 60elt) and 50% of both contributions (50ste / elt), were determined.

The ZYU ligand presented higher values of similarity of overlap with caffeine at the 100ste, 60ste/40elt and 50ste/elt levels (0.8967, 0.6860 and 0.6476, respectively), second higher values of 40ste/60elt (0.6098) and median value for 100elt (0.4818). The closer to 1 the values are, the greater the degree of similarity between the binder and the caffeine. While, in contrast, for smaller values, the greater the degree of structural difference [24].

The results for overlap similarity allow us to consider the ZYU ligand with a high degree of similarity with caffeine. This ligand complexed to the Chk1 receptor, is available from the PDB code 2WMU, and its IUPAC name is 6-morpholine-4-yl-9H-purine. Fig. **9** shows the overlap of ZYU with caffeine.

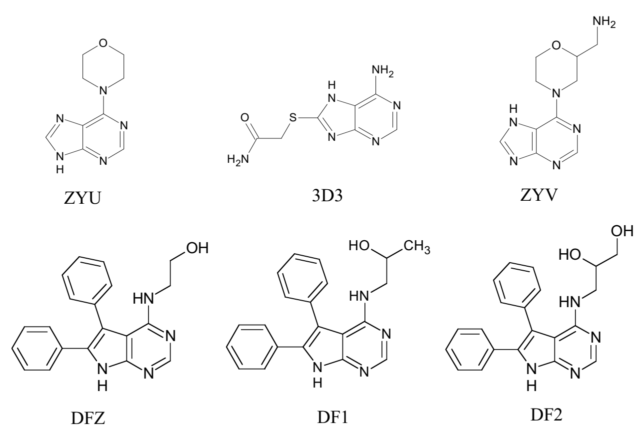

Fig. (8). Structure of the complexed ligands with Chk1 selected from PDB.

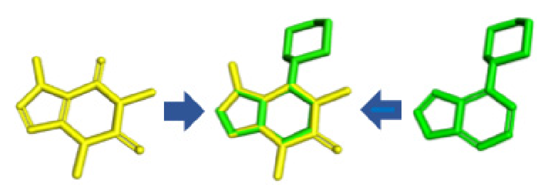

Fig. (9). Caffeine overlap (yellow) with ZYU ligand (green). (The color version of the figure is available in the electronic copy of the article).

3.5.2 Validation and Molecular Docking

The comparison between the conformations of the crystallographic ligand (complexed with Chk1 and experimental values of crystallography) with the computational data resulting from the redocking (RMSD = 0.570), shows that the parameters used in the docking protocol were representative. RMSD values below the

Table 12. Overlap similarity values of the ligands analyzed.

Complex	Ligand	Overlap				
PDB Code	PDB Code	100ste	100elt	60ste/40elt	40ste/60elt	50ste/elt
2WMU	ZYU	0.8967	0.4818	0.6860	0.6098	0.6476
2CGX	3D3	0.8349	0.5361	0.6068	0.6226	0.5645
2WMV	ZYV	0.8138	0.3378	0.5865	0.4969	0.5384
2BRM	DFZ	0.7152	0.5368	0.5709	0.5852	0.5503
2BRN	DF1	0.6874	0.4597	0.6244	0.5991	0.6131
2BRO	DF2	0.6658	0.3912	0.5616	0.4997	0.5408

100ste = 100% of steric contribution; 100elt = 100% of electrostatic contribution; 60ste/40elt = 60% steric and 40% electrostatic; 40ste/60elt = 40% steric and 60% electrostatic; and 50ste/50elt = 50% of both contribution.

tolerance level of up to 2.0 Å are considered to be of good quality [54, 55]. The alignment between experimental and computational conformations, which qualitatively shows this result, can be seen in Fig. **10**.

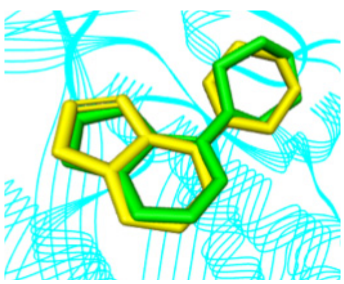

Fig. (10). Comparison between crystallographic ligand pose (in green) and the top-ranked pose resulting from docking (yellow). (The color version of the figure is available in the electronic copy of the article).

The interactions resulting from the docking pose of the ZYU with the Chk1 receptor were: two hydrogen bonds with CYS87 and GLU85, and four carbon-hydrogen bonds with CYS87, GLU91, LEU15 and GLY16, in a total of six interactions. Fig. **11** shows the interactions of ZYU with Chk1.

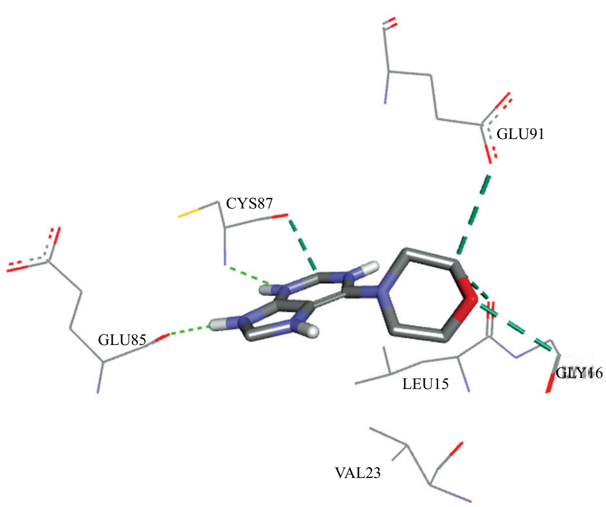

Fig. (11). Interactions between the ZYU ligand and the Chk1 receptor, calculated by Autodock 4.2.6.

The parameters related to the dimensions of the grid box and coordinates of the ligand's center, used in the docking validation, were applied to the reference molecules (caffeine and molecule 03), ZINC08992920 and ZINC08706191.

Fig. **12** shows the interactions for individually docked molecules. Caffeine showed two carbon-hydrogen bonds, with GLU85 and CYS87, and a pi-sigma bond with LEU15, with three interactions in total. The molecule 03 showed two hydrogen bonds with CYS87, one carbon-hydrogen bond with TYR86 and two pi-sigma bonds, with LEU137 and LEU15, in a total of five interactions. The molecule ZINC08992920 interacted with the receptor through two hydrogen bonds, with CYS87 and GLU91, one carbon-hydrogen bond with CYS87 and two pi-sigma bonds with LEU137 and LEU15, in a total of five interactions. The molecule ZINC08706191 interacted with two hydrogen bonds with CYS87 and GLU91, one carbon-hydrogen bond with CYS87 and two pi-sigma bonds with LEU15, in a total of five interactions.

Quantitative data of distances and binding free energies (BFE) between the ligands and the Chk1 receptor can be seen in Table **13**. It is possible to verify that, among the reference molecules (caffeine and molecule 03), the increase in the number of interactions resulted in the lowering of free binding energy, which indicates a higher degree of spontaneity of the interactions. This effect is noticeable in molecules ZINC08992920 and ZINC08706191 with five interactions each and smaller binding energies than the reference molecules. Common interactions with the amino acids CYS87 and LEU15 occurred in all molecules analyzed, indicating that they have key importance in the epithelial anticancer activity.

It is noted that the pi-sigma interaction with LEU15 and LEU137 on molecules 03, ZINC08992920 and ZINC08706191, attributed lower BFE to these three molecules when compared to the interactions and BFE of ZYU and caffeine that have no Pi-sigma interactions with none of these amino acids.

Comparing the molecules ZINC08992920 and ZINC08706191, we can observe the lowering of the free energy of binding (-7.41) in ZINC08706191 that has two interactions with LEU15 in respect to the BFE (-7.13) in ZINC08992920, that has a Pi-sigma interaction with LEU15 and LEU137, indicating that the interaction with LEU15 is a favorable factor for lowering BFE between these two molecules. The pi-sigma interactions have strong hydrophobic characteristic, and when related to favorable entropic factors can promote the lowering of the free energy of ligand-receptor binding [56].

It is interesting to note that, due to structural similarity, the numerical values of the pharmacophoric characteristics, pharmacokinetics properties and the activity values calculated by the MLR models were similar for the molecules ZINC08992920 and ZINC08706191 (see Table **14**), which resulted in approximate values of BFE, due to the interactions similarity.

Caffeine

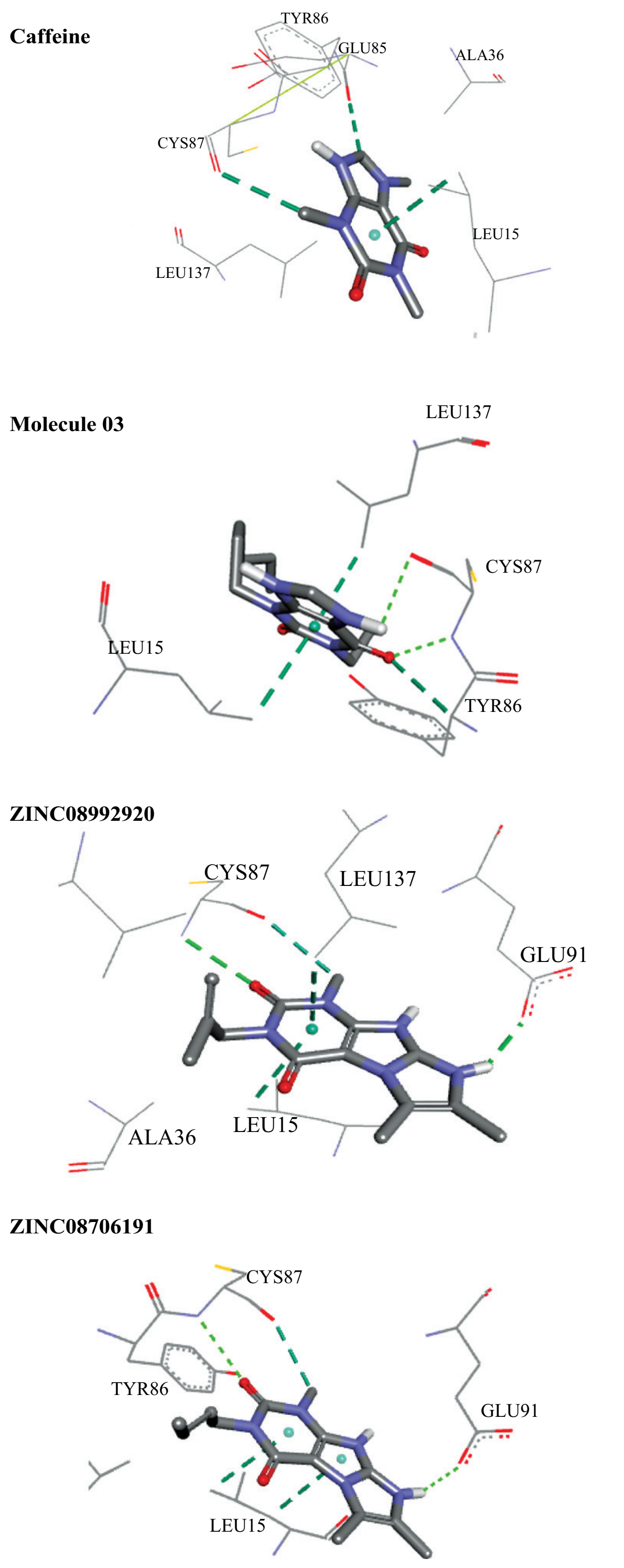

Fig. (12). Interactions between the best screened molecules and the Chk1 receptor calculated by Autodock 4.2.6.

3.5.3. Correlation Between Pharmacophoric Properties, Pharmacokinetics and $pICT_{50}$ with BFE

Correlations between pharmacophoric, pharmacokinetic properties as well as the calculated $pICT_{50}$ with BFE (Table **14**) showed negative values for all analyzed variables, which indicate an inverse proportionality relationship between them and BFE. These results are consistent with the significance of each analyzed variable, which allows us to consider that an increase in the values of the pharmacophoric properties, HIA and PPB promotes increase of the activity and decrease of BFE.

The low correlation with BBB (-0.02) indicates that the value of BFE has no respect to this property, as expected, since this variable is related to CNS side effects, signalizing that molecules ZINC08992920 and ZINC08706191 do not show such effect.

The calculated $pICT_{50}$ values and their correlations with BFE for the molecules ZINC08992920 and ZINC08706191, the mono (Eq1) and bi (Eq2) parametric models, with correlations -0.89 and -0.90, respectively, have a higher correlation with the BFE values than the tri (Eq3) and tetra (Eq4) parametric models, which is consistent with the activity observed for these molecules predicted by the mono and bi parametric models.

CONCLUSION

The virtual screening performed here showed reliable results in all its stages. The MLR models built from the pharmacophoric data were classified with excellent statistical quality, due to the high values of R, R^2, R_A^2 and low SEE values, and good statistical significance confirmed by the t-test, with emphasis on the tetra-parametric model, considered the best model. The validation of the MLR models indicated excellent predictive power of the models, indicated by the low values of errors in both the predictions for the training set and the test set. These results were also qualified by the good correlations between experimental and calculated $pICT_{50}$ values.

The pharmacophore model inserted in the ZINCPharmer webserver aided us to select 350 molecules, and subsequently 24 were selected using the BindingDB by Tanimoto similarity. The low amount of molecules found from the virtual screening in this webserver evidences the quality of the analytical filters used in the screening.

The pharmacokinetic properties indicated in general better results than the reference values and limits available in the literature, with HIA values higher than 90% and PPB (considered prediction errors) within the limits of clinical significance. BBB also indicated good results, where only molecules 03 (reference) and ZINC08990240 showed possible effects on the CNS.

The molecules ZINC08992920 (3 hits of toxicity, with mutagenicity and carcinogenicity alerts) and ZINC08706191 (1 hit of toxicity, only with one mutagenicity alert) presented lower toxicities among all the tested molecules. The attested mutagenicity needs to be better evaluated (*in vitro* e *in vivo* tests), because mutagenicity may have an effect depending on the level of consumption or dose of administered substance.

BFE values correlated to the properties analyzed show that BBB has no respect to BFE values, as expected, due to the low BBB values observed and this indicates side effect. High negative correlations between BFE and pharmacophoric properties, HIA, PPB, $pICT_{50}$ calculated by Eq1 and by Eq2, indicate that these properties are fundamentally related to the low BFE values.

Results here obtained and discussed, which sought to evaluate the potential epithelial anticancer activity of the screened molecules, allowed us to classify the molecules ZINC08992920 and ZINC08706191 as the best ones along the observed series, and to point to ZINC08706191 (presented minor hit in toxicity) as the best among all. However, these two molecules can subsequently be

Table 13. Distances and BFE between ligands and Chk1.

Molecule	Aminoacid	Distance (Å)	Type	BFE (kcal mol^{-1})
ZYU	CYS87	2.865	Hydrogen bond	-5.37
	CYS87	3.302	Carbon-hydrogen bond	
	GLU85	1.730	Hydrogen bond	
	GLU91	3.402	Carbon-hydrogen bond	
	LEU15	3.515	Carbon-hydrogen bond	
	GLY16	3.236	Carbon-hydrogen bond	
Caffeine	GLU85	2.916	Carbon-hydrogen bond	-5.14
	CYS87	2.940	Carbon-hydrogen bond	
	LEU15	3.528	Pi-sigma	
Molecule 03	CYS87	2.879	Hydrogen bond	-5.90
	CYS87	2.401	Hydrogen bond	
	TYR86	2.985	Carbon-hydrogen bond	
	LEU137	3.560	Pi-sigma	
	LEU15	3.581	Pi-sigma	
ZINC08992920	CYS87	2.911	Hydrogen bond	-7.13
	CYS87	3.337	Carbon-hydrogen bond	
	GLU91	2.007	Hydrogen bond	
	LEU137	3.753	Pi-sigma	
	LEU15	3.867	Pi-sigma	
ZINC08706191	CYS87	2.947	Hydrogen bond	-7.41
	CYS87	3.165	Carbon-hydrogen bond	
	GLU91	2.428	Hydrogen bond	
	LEU15	3.836	Pi-sigma	
	LEU15	3.930	Pi-sigma	

Table 14. Correlation between the variables analyzed and BFE.

	Pharmacophoric Characteristics				Pharmacokinetic Properties			Calculated pICT$_{50}$				
Molecule	**A**	**GF**	**SF**	**Hyd**	**HIA%**	**PPB%**	**BBB**	**Eq1**	**Eq2**	**Eq3**	**Eq4**	**BFE**
Caffeine	24	9	9	0	93.82	14.07	0.33	0.58	0.73	0.44	0.63	-5.14
Molecule 03	39	13	12	6	88.13	75.91	1.60	1.37	1.44	1.44	1.52	-5.90
ZINC08992920	37	14	14	6	97.53	63.15	0.80	1.57	1.65	1.20	1.25	-7.13
ZINC08706191	37	14	14	6	97.53	64.25	0.65	1.57	1.65	1.20	1.25	-7.41
CoBFE	-0.70	-0.89	-0.96	-0.79	-0.66	-0.64	-0.02	-0.89	-0.90	-0.61	-0.54	

A = number of atoms; GF = General Characteristics; SF = Spatial Characteristics; Ar = Aromatic; Hyd = Hydrophobic; HIA% = Human Intestinal Absorption; PPB = Plasma Protein Binding; BBB = Blood Brain Barrier.

subjected to further analysis to a better evaluation of their pharmacological potential against epithelial cancer.

ETHICS APPROVAL AND CONSENT TO PARTICIPATE

Not applicable.

HUMAN AND ANIMAL RIGHTS

No Animals/Humans were used for studies that are base of this research.

CONSENT FOR PUBLICATION

Not applicable.

CONFLICT OF INTEREST

The authors declare no conflict of interest, financial or otherwise.

ACKNOWLEDGEMENTS

We acknowledge the support provided by the PROPESP/UFPA. To the Postgraduate Program in Biodiversity and Biotecnoloy of Amazon (PPG-Bionorte), Paraense Museum Emilio Goeldi (MPEG). Laboratory of Molecular Modeling and Simulation System of Federal Rural University of Amazônia (UFRA-Brazil) and Computational Laboratory of Pharmaceutical Chemistry, Faculty of Pharmaceutical Sciences of Ribeirão Preto, University of São Paulo, Ribeirão Preto (USP/RP) for computational support. To Elias Carvalho Padilha for his assistance in the revision of the English language.

REFERENCES

[1] Rosenberg SA. Progress in human tumour immunology and immunotherapy. Nature 2001; 411(6835): 380-4.

[2] Cairns J. The origin of human cancers. Nature 1981; 289 (5796): 353-7.

[3] Brentani RR, Chammas R, Coelho FRG. Mecanismos de invasão e metástases. In: Brentani MN, Coelho FRG, Iyeyasu H, Kowalski LP, Eds. Bases da Oncologia. 1st ed. São Paulo: Livraria e Editora Marina, 1998; pp. 1-21.

[4] WHO - World Health Organization. World Cancer Report 2014. Available from: www.who.int/cancer/ [cited: 25th Sep 2016].

[5] Popim RC, Corrente JE, Marino JAG, Souza CA. Skin cancer: use of preventive measures and demographic profile of a risk group in the city of Botucatu. Cien Saude Colet 2008; 13(4): 1331-6.

[6] Almeida JRC. Farmacêuticos em oncologia: uma nova realidade. São Paulo: Atheneu, 2004.

[7] Sarkaria, JN, Busby EC, Tibbetts RS, *et al*. Inhibition of ATM and ATR kinase activities by the radiosensitizing agent, caffeine. Cancer Res 1999; 59(17): 4375-82.

[8] Lu YP, Lou YR, Peng QY, *et al*. Effect of Caffeine on the ATR/Chk1 Pathway in the Epidermis of UVB-Irradiated Mice. Cancer Res 2008; 68(7): 2523-9.

[9] Rogozin EA, Lee KW, Kang NJ, *et al*. Inhibitory effects of caffeine analogues on neoplastic transformation: structure–activity relationship. Carcinogenesis 2008; 29(6): 1228-34.

[10] Alves AB. Simultaneous determination of theobromine, theophylline and caffeine in teas by high performance liquid chromatography. Braz J Pharm Sci 2002; 38(2): 237-43.

[11] Kandakatla N, Ramakrishnan G. Ligand Based Pharmacophore Modeling and Virtual Screening Studies to Design Novel HDAC2 Inhibitors. Adv Bioinformatics 2014; 2014:812148.

[12] Starosyla SA, Volynets GP, Bdzhola, VG, Golub AG, Protopopov MV, Yarmoluk SM. ASK1 pharmacophore model derived from diverse classes of inhibitors. Bioorg. Med. Chem Lett 2014; 24(18): 4418-23.

[13] ACD/Chemsketch Freeware, version 12.00: Advanced Chemistry Development, Inc, Toronto, ON, Canada, 2010.

[14] BABEL, Open. The open source chemistry toolbox. 2011.

[15] ChemPlus, Modular Extensions to HyperChem, Release 6.02. Gainesville: Molecular Modeling for Windows Hyper Inc. 2000.

[16] Schneidman-Duhovny D, Dror O, Inbar Y, Nussinov R, Wolfson HJ. PharmaGist: a webserver for ligand-based pharmacophore detection. Nucleic Acids Res 2008; 36: 223-8.

[17] Schneidman-Duhovny D, Dror O, Inbar Y, Nussinov R, Wolfson HJ. Deterministic Pharmacophore Detection by Multiple Flexible Alignment of Drug-Like Molecules. J Comput Biol 2008; 15(7): 737-54.

[18] Santos CBR, Lobato CC, Braga FS, *et al*. Rational Design of Antimalarial Drugs Using Molecular Modeling and Statistical. Curr Pharm Des 2015; 21(28): 4112-27.

[19] STATISTICA (Data Analysis Software System); Version 6.1, StatSoft, Inc., 2004.

[20] Koes DR, Camacho CJ. ZINCPharmer: pharmacophore search of the ZINC database. Nucleic Acids Res 2012; 40: 409-14.

[21] John J. Irwin and Brian K. Shoichet. ZINC – A Free Database of Commercially Available Compounds for Virtual Screening, J Chem Inf Model. 2005; 45(1): 177-82.

[22] Liu, T.; Lin, Y.; Wen X.; Jorissen R. N.; Gilson, M. K.; BindingDB: a web-accessible database of experimentally determined protein–ligand binding affinities. Nucleic Acids Res 2007; 35: 198-201.

[23] Sanderson DM, Earnshaw CG. Computer prediction of possible toxic action from chemical structure; the DEREK system. Hum Exp Toxicol 1991; 10 (4): 261-73.

[24] Dassault Systèmes BIOVIA. Discovery studio modeling environment. San Diego, CA: Dassault Systèmes, 2015.

[25] PDB – Protein Data Bank. Available from: http://www.ncbi.nlm.nih.gov/protein/ [cited: 20th Oct 2016].

[26] Matthews TP, Klair S, Burns S, *et al*. Identification of Inhibitors of Checkpoint Kinase 1 Through Template Screening. J. Med. Chem., 2009; 52(15): 4810-19.

[27] Morris GM, Goodsell DS, Halliday RS, *et al.* Automated Docking Using a Lamarckian Genetic Algorithm and and Empirical Binding Free Energy Function. J Comput Chem 1998; 19(14): 1639-62.

[28] Agrawal R, Jain P, Dikshit SN, Bahare RS, Ganguly S. Ligand-based pharmacophore detection, screening of potential pharmacophore and docking studies, to get effective glycogen synthase kinase inhibitors. Med Chem Res 2013 22(11): 5504-35.

[29] Gupta S, Mohan CG. Dual binding site and selective acetylcholinesterase inhibitors derived from integrated pharmacophore models and sequential virtual screening. Biomed Res Int 2014, Volume 2014: 1-21.

[30] Sakkiah, S.; Lee, K. W.; Pharmacophore-based virtual screening and density functional theory approach to identifying novel butyrylcholinesterase inhibitors. Acta Pharmacol Sin 2012; 33(7): 964-78.

[31] Liu T, Lin Y, Wen X, Jorissen RN, Gilson MK. BindingDB: a web-accessible database of experimentally determined protein–ligand binding affinities. Nucleic Acids Res 2007; 35: 198-201.

[32] CSIZMADIA, F. JChem: Java applets and modules supporting chemical database handling from web browsers. J Chem Inf Comput Sci 2000; 40(2): 323-4.

[33] Willett P, Barnard JM, Downs GM. Chemical similarity searching. J Chem Inf Comput Sci 1998; 38(6): 983-96.

[34] Souza J, Feitas ZMF, Storpirtis S. In vitro models for the determination of drug absorption and a prediction of dissolution/absorption relationships. Braz J Pharm Sci 2007; 43(4): 515-27.

[35] Wang J, Hou T. Recent Advances on in silico ADME Modeling. Annu Rep Comput Chem 2009; 5: 101-27.

[36] Richard TS. Protein binding: What does it mean? DICP 1989; 23(7-8 Suppl): 27-31.

[37] Wilkinson GR. Plasma and tissue binding considerations in drug disposition. Drug Metab Rev 1983; 14(3):427-65.

[38] Rowland M. Protein binding and drug clearance. Clin Pharmacokinet 1984; 9(suppl): 10-7.

[39] Blanchard J. Protein binding of caffeine in young and elderly males. J Pharm Sci 1982; 71(12): 1415-18.

[40] Fausch K, Uehlinger DE, Jakob S, Pasch A. Haemodialysis in massive caffeine intoxication. Clin Kidney J 2012; 5(2): 150-2.

[41] Zylber-Katz E, Granit L, Levy M. Relationship between caffeine concentrations in plasma and saliva. Clin Pharmacol Ther 1984; 36(1): 133-7.

[42] Rojas H, Ritter C, Pizzol FD. Mechanisms of dysfunction of the blood-brain barrier in critically ill patients: emphasis on the role of matrix metalloproteinases. Rev Bras Ter Intensiva 2011; 23(2): 222-7.

[43] Ma X, Chen C, Yang, J. Predictive model of blood-brain barrier penetration of organic compounds. Acta Pharmacol Sin 2005; 26(4): 500-12.

[44] Liu J, Shen B, Shi M, Cai J. Higher caffeinated coffee Intake is associated with reduced malignant melanoma risk: A meta-nnalysis study. PLoS ONE 2016; 11(1): e0147056.

[45] Silva NSR, Santos CF, Gonçalves LKS, *et al.* Molecular modeling of the major compounds of sesquiterpenes class in copaiba oil-resin. Br J Pharm Res 2015; 7(4): 247-63.
[46] Vieira JB, Braga FS, Lobato CC, *et al*. A QSAR, pharmacokinetic and toxicological study of new artemisinin compounds with anticancer activity. Molecules 2014; 19(8): 10670-97.
[47] Woo YT. Mechanisms of action of chemical carcinogens, and their role in structure-activity relationships (SAR) analysis and risk assessment. In: Benigni R, ed, Quantitative Structure-Activity Relationship (QSAR) Models of Mutagens and Carcinogens, Boca Raton: CRC Press 2003.
[48] Primo MS, Calliari CM, Castro-Gómez RJH, Mauro MO, Mantovan MS, Oliveira RJ. Assessment of mutagenicity and antimutagenicity of a biopolymer extracted from the microorganism Agrobacterium radiobacter in mice. Braz J Pharmacog 2010; 20(3): 340-7.
[49] Mauro MO, Pesarini JR, Ishii PL, Silva Ariane F, Oliveira RJ. Chemopreventive activity of phenylalanine against damage mutagenic prompted by the acute administration of cyclophosphamide in pregnant and non-pregnant mice using the micronucleus test. Braz J Pharmacog 2010; 20(3): 334-9.
[50] Basketter DA. Skin sensitization: Strategies for the assessment and management of risk. Br J Dermatol 2008; 159(2): 267-73.
[51] Cronin MT, Basketter DA. Multivariate QSAR analysis of a skin sensitization database. SAR QSAR Environ Res 1994; 2(3): 159-79.
[52] Nehlig A, Debry G. Potential genotoxic, mutagenic and antimutagenic effects of coffee: A review. Mutat Res 1994; 317(2): 145-62.
[53] Kuhlmann W, Fromme HG, Heege EM, Ostertag W. The mutagenic action of caffeine in higher organisms. Cancer Res 1968; 28(11): 2375-89.
[54] Hevener KE, Zhao W, *et al*. Validation of molecular docking programs for virtual screening against dihydropteroate synthase. J Chem Inf Model 2009; 49(2): 444-60.
[55] Gowthaman U, Jayakanthan M, Sundar D. Molecular docking studies of dithionitrobenzoic acid and its related compounds to protein disulfide isomerase: computational screening of inhibitors to HIV-1 entry. BMC Bioinformatics 2008, 9(Suppl 12): 14.
[56] Berg JM, Tymoczko JL, Stryer L. Biochemistry. 5th edition. New York: W H Freeman; 2002. Section 1.3, Chemical Bonds in Biochemistry.